Machine learning-accelerated computational solid mechanics: Application to linear elasticity

Rajat Arora*

Abstract

This work presents a novel physics-informed deep learning based super-resolution framework to reconstruct high-resolution deformation fields from low-resolution counterparts, obtained from coarse mesh simulations or experiments. We leverage the governing equations and boundary conditions of the physical system to train the model without using any high-resolution labeled data. The proposed approach is applied to obtain the super-resolved deformation fields from the low-resolution stress and displacement fields obtained by running simulations on a coarse mesh for a body undergoing linear elastic deformation. We demonstrate that the super-resolved fields match the accuracy of a numerical solver running at 400 times coarse mesh resolution, while simultaneously satisfying the governing laws.

1 Introduction

Image super-resolution (SR) is an active area of research in the field of computer science which aims at recovering high-resolution (HR) image from a low-resolution (LR) image. In this work, we focus on exploring the concept of image super-resolution to develop a physics-informed Deep Learning (DL) model to reconstruct HR deformation fields (stress and displacements) from LR fields without requiring any HR labeled data. The LR data could be obtained by running simulations on a coarse mesh or from experiments such as digital image correlation. The overall schematic of the proposed physics-informed strategy for super resolution is depicted in Fig. 1. The use of such physics-informed SR framework will allow researchers to solve computationally expensive simulations much faster and enable them to increase accuracy without additional costs.

Recently, several researchers have explored the possibility of using deep learning based super-resolution to reconstruct HR fluid flow fields from LR (possibly noisy) data. The data-driven approaches for reconstructing HR flow field [FFT21, FFT19, DHLK19, BGL+19, XFCT18] relies on the availability of large amount of HR labeled data. Moreover, the HR field obtained from data-driven approaches may fail to satisfy physics-based constraints

*Research Scientist at Siemens Technology. rajat.arora9464@gmail.com.

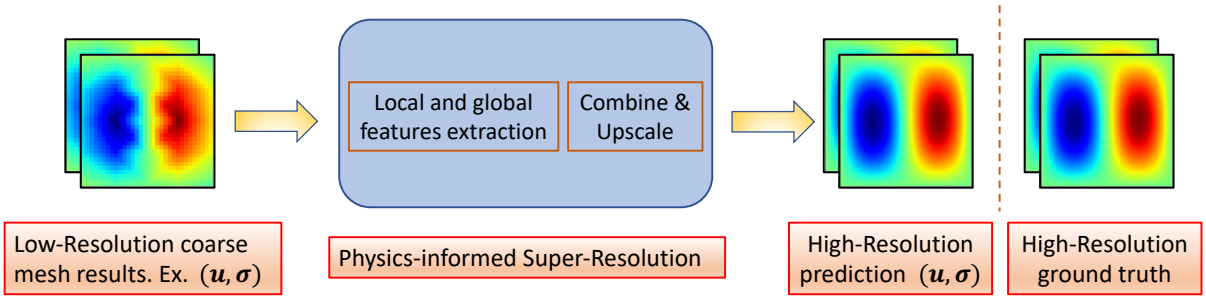

Figure 1: Schematic of the super-resolution framework.

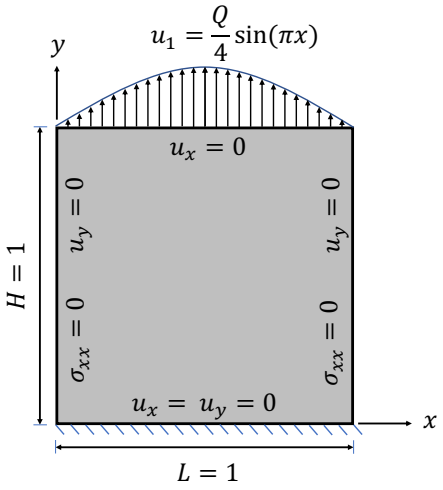

Figure 2: Schematic showing the geometry and the applied boundary conditions.

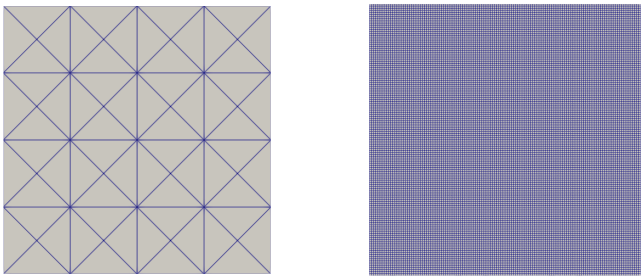

(a) Coarse triangular mesh with 41 nodes.

(b) 128×128 structured mesh with 16384 nodes.

Figure 3: Coarse and fine meshes for the low-resolution input data and super-resolved output, respectively.

because of the lack of any embedded physical constraints in the model itself. Several studies have demonstrated the merits of developing physics-informed DL models for SR in the fluid mechanics community [EAK+20, SWB+20, SW20, GSW21]. However, to the best of author's knowledge, developing an effective physics-informed DL model for super-resolution in label-scarce or label-free scenarios for solid mechanics problems has not yet been explored.

The layout of the rest of this paper is as follows: In Sec. 2, a brief review of the governing equations for modeling elastic deformation in solids is presented. Model architecture and construction of loss function are discussed in Secs. 3 and 4, respectively. Sec 5 presents the findings for the evaluation of the proposed SR-framework after briefly discussing simulation setup and data collection strategy. Conclusions and future opportunities are presented in Sec. 6.

2 Governing Equations for Elasticity

The governing equations for elasticity problems, in the absence of inertial forces, is written as follows:

$$\begin{aligned} Div\boldsymbol{\sigma} + \boldsymbol{B} &= \boldsymbol{0}, \quad \text{in} \quad \Omega, \\ \boldsymbol{\sigma} = \mathbb{C} : \boldsymbol{\epsilon}, \quad \boldsymbol{\epsilon} &= \frac{1}{2}\left(\nabla \boldsymbol{u} + (\nabla \boldsymbol{u})^T\right) \\ \boldsymbol{\sigma}\boldsymbol{n} = \boldsymbol{t}_{bc} \quad &\text{on} \quad \partial\Omega_N \quad \text{and} \quad \boldsymbol{u} = \boldsymbol{u}_{bc} \quad \text{on} \quad \partial\Omega_D, \end{aligned} \tag{1}$$

In the above, $\boldsymbol{\sigma}$ and $\boldsymbol{\epsilon}$ denotes the stress and the (linearized) strain in the material. $\boldsymbol{u}$ and $\boldsymbol{B}$ denotes the displacement vector and body force vector per unit volume, respectively. Ω denotes the volumetric domain, Div denotes the divergence operator, and $\mathbb{C}$ is the fourth order elasticity tensor. $\boldsymbol{t}_{bc}$ and $\boldsymbol{u}_{bc}$ denote the known traction and displacement vectors on the (non-overlapping) parts of the boundary $\partial\Omega_N$ and $\partial\Omega_D$, respectively. $\boldsymbol{n}$ denotes the unit outward normal on the external boundary $\partial\Omega$. Under two-dimensional plane-strain conditions, the unknown components for displacement vector and stress tensor are (u_x, u_y) and (σ_{xx}, σ_{yy}, σ_{xy}), respectively.

3 Model Architecture

We develop and train a physics-informed DL framework to approximate the mapping $\Psi : \mathcal{I}^{LR} \rightarrow \mathcal{I}^{HR}$ to reconstruct the HR deformation field ($\mathcal{I}^{HR}$) from the LR ($\mathcal{I}^{LR}$) data obtained from experiments or coarse mesh simulations. We adopt the Residual Dense Network (RDN) proposed in [ZTK+18] to extract and adaptively fuse features from all the layers in the LR space. In this work, we use the following hyper-parameters for the RDN model: number of layers: 4, growth rate 32, number of residual blocks 2, and number of features 32.

4 Constructing the Loss Function

For the unsupervised model, wherein the HR labeled data is not needed, the total network loss $\mathcal{L}$ is obtained only from the physics-based constraints corresponding to the governing equations and boundary conditions. For the mixed-variable formulation (displacement vector $\boldsymbol{u}$ and stress tensor $\boldsymbol{\sigma}$ as outputs), the total loss function $\mathcal{L}$ is constructed as follows

$$\begin{aligned} \mathcal{L} = &\lambda_1 \underbrace{||\nabla \cdot \boldsymbol{\sigma}||}_{\text{PDE}} + \lambda_2 \underbrace{||\boldsymbol{\sigma} - \mathbb{C} : \boldsymbol{\epsilon}||}_{\text{Constitutive law}} \\ &+ \lambda_3 \underbrace{||\boldsymbol{u} - \boldsymbol{u}_{bc}||_{\partial\Omega_U}}_{\text{Dirichlet BC}} + \lambda_4 \underbrace{||\boldsymbol{\sigma}\boldsymbol{n} - \boldsymbol{t}_{bc}||_{\partial\Omega_N}}_{\text{Neumann BC}}, \end{aligned} \tag{2}$$

where $||(\cdot)||$ denotes the L^1 norm of the quantity $(\cdot)$. L^1 norm is chosen to make the model robust to noise and outliers in the LR data. The scalar constants λ_1, λ_2, λ_3, and λ_4 are

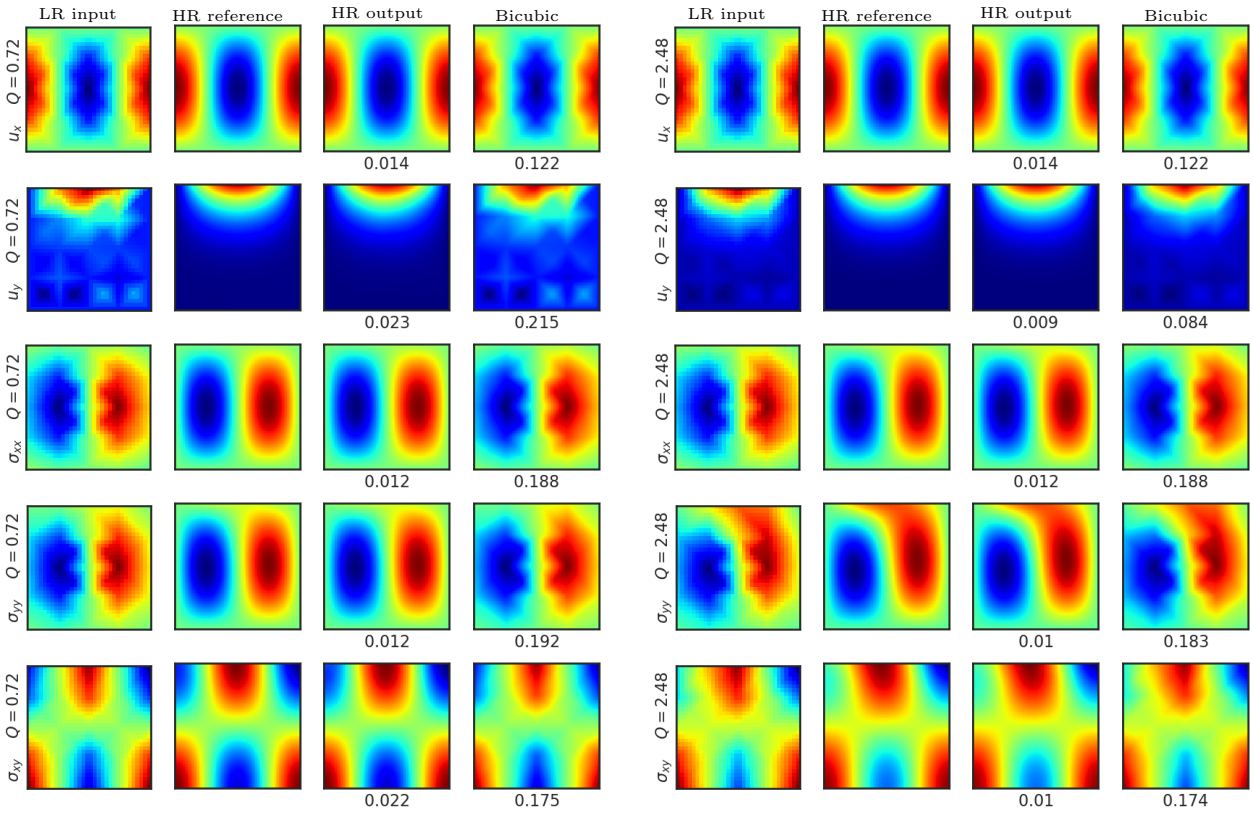

Figure 4: The color contours of displacement vector and stress tensor in two-dimensional elastic deformation reconstructed with machine-learned super-resolution. Values below the plots indicate the L_2 error e. In both the blocks, the LR input data, HR reference, SR output, and bicubic interpolation are plotted from the left to the right.

chosen to nondimensionalize the individual loss components. In this work, we choose $\lambda_1 = \frac{H}{\mu}$, $\lambda_2 = \frac{1}{\mu}$, $\lambda_3 = \frac{20}{U_0}$, and $\lambda_4 = \frac{20}{\mu}$, where μ and U_0 represent the shear modulus and the characteristic displacement in the body, respectively. H denotes the height of the body. Relatively larger magnitudes of λ_3 and λ_4 are chosen to assign more weight to the boundary conditions.

The neural network is implemented and trained using PyTorch framework [PGM+19]. The network's total loss $\mathcal{L}$ is minimized by iteratively updating trainable parameters by using Adam optimizer [KB15] for around 2000 epochs with learning rate $\eta = 10^{-4}$. We also use `ReduceLROnPlateau` scheduler with the `patience` = 30. L-BFGS algorithm [ZBLN97] is then used for another 2000 epochs for local fine-tuning of solution. The source code and the dataset used in this research can be found at https://github.com/sairajat/SR_LE upon acceptance of this paper.

5 Results & Discussion

In what follows, we demonstrate the effectiveness of SR framework in reconstructing HR displacement and stress fields from LR input data for linear elastic simulations – which we believe is a first step in demonstrating the strength of machine-learned super-resolution techniques in solid mechanics.

We apply the framework to resolve the stress and displacement fields within an isotropic body undergoing linear elastic deformation. The schematic of the body along with the boundary conditions is shown in Figure 2. The body is assumed to deform quasi-statically under plane strain conditions with the body force vector $\boldsymbol{B}$ given as

$$\begin{aligned} B_x &= \lambda \left[4\pi^2 \cos(2\pi x)\sin(\pi y) - \pi \cos(\pi x) Q y^3\right] \\ &\quad + \mu \left[9\pi^2 \cos(2\pi x)\sin(\pi y) - \pi \cos(\pi x) Q y^3\right], \\ B_y &= \lambda \left[2\pi^2 \sin(2\pi x)\cos(\pi y) - 3\sin(\pi x) Q y^2\right] \\ &\quad + \mu \left[-6\sin(\pi x) Q y^2 + 2\pi^2 \sin(2\pi x)\cos(\pi y)\right. \\ &\quad \left. + 0.25\pi^2 \sin(\pi x) Q y^4\right]. \end{aligned}$$

In this work, the material constants λ and μ are taken to be 1 and 0.5, respectively. The quantity $Q \in [0, 4]$ affects the boundary conditions (see Fig. 2) and the applied body force. The characteristic displacement U_0 is taken to 1 (maximum value of u_y on the boundary). The ground truth data is generated by solving the system of equations (1) on a coarse mesh (shown in Fig. 3a) using Finite Element Method for Q regularly sampled at an interval of 0.04. The data is then randomly split in a $80:20$ ratio for training and test purposes.

The framework super-resolves the deformation fields onto the 128×128 mesh, shown in Fig. 3b, which is ≈ 400 times finer than the coarse mesh used to obtain the LR data. The input to the model comprises 2-d arrays of LR displacement vector and LR stress tensor components. The corresponding HR outputs are obtained by doing a forward pass through the trained model. For comparison, along with HR data, we also utilize a simple bicubic interpolation of fields. We note that the HR labeled data is used only for the comparison with the predicted outputs.

Figure 4 presents the results for the reconstructed displacement and stress fields for 2 different values of Q. We can see that the framework is able to super-resolve all the deformation fields with great accuracy as the plots show great agreement with the reference HR ground truth data. To qualitatively measure the accuracy, we define a relative error measure as $e = \frac{||\mathcal{I}^{HR} - \mathcal{I}^{LR}||_{L^2}}{||\mathcal{I}^{HR}||_{L^2}}$. The values of e are reported underneath the reconstructed fields obtained using the SR framework and the bicubic interpolation. As can be seen, the error is larger for the bicubic interpolated data as compared to the HR output from the physics-informed model. This validates the ability of the physics-informed SR framework to faithfully reconstruct the fields at a higher resolution while simultaneously satisfying the governing laws. Therefore, we successfully trained and demonstrated a physics-informed super-resolution framework to reconstruct high-resolution stress and displacement fields from low-resolution simulation data with large discretization errors. We note that the proposed physics-informed

SR framework can be easily extended to non-rectangular domains [GSW20] or account for boundary conditions in a *hard* manner [RSL21].

6 Conclusion

In summary, we successfully trained and evaluated a physics-informed super-resolution framework based on Residual Dense Network (RDN) [ZTK+18] to resolve the deformation fields in a body undergoing elastic deformation. The method learns high-resolution spatial variation of displacement and stress fields for the linear elastic calculations and matches the accuracy of an advanced numerical solver running at 400× the coarse mesh resolution (see Fig. 3 and 4) for the linear elastic case discussed. These advantages are possible due to the combined effect of two rapidly evolving research areas - Physics informed neural networks [RPK17, RPK19] and computer vision [VDDP18]. We emphasize that the current work focuses on the demonstration of feasibility of the concept while the assessment of potential computational advantages, including the extension to hyperelastic deformation, is deferred to future research.

The approach exemplifies how machine-learning can be leveraged to conduct such mechanical calculations for materials with complex constitutive response (eg. dislocation mediated plastic deformation and fracture modeling [AZA20, NN19, NT19, AA20, YZL+16, Aro19, KT08, LNN19, AZA20, BHLV14]) to reduce the computational complexity and accelerate scientific discovery and engineering design.

Acknowledgments

This work was conceptualized during the author's time at Carnegie Mellon University (CMU). The author thank Ankit Shrivastava, Ph.D. candidate at CMU, for useful discussions and comments on the manuscript.

References

[AA20] Rajat Arora and Amit Acharya. Dislocation pattern formation in finite deformation crystal plasticity. *International Journal of Solids and Structures*, 184:114–135, 2020.

[Aro19] Rajat Arora. *Computational Approximation of Mesoscale Field Dislocation Mechanics at Finite Deformation*. PhD thesis, Carnegie Mellon University, 2019.

[AZA20] Rajat Arora, Xiaohan Zhang, and Amit Acharya. Finite element approximation of finite deformation dislocation mechanics. *Computer Methods in Applied Mechanics and Engineering*, 367:113076, 2020.

[BGL+19] Mathis Bode, Michael Gauding, Zeyu Lian, Dominik Denker, Marco Davidovic, Konstantin Kleinheinz, Jenia Jitsev, and Heinz Pitsch. Using physics-informed super-resolution generative adversarial networks for subgrid modeling in turbulent reactive flows. *arXiv preprint arXiv:1911.11380*, 2019.

[BHLV14] Michael J Borden, Thomas JR Hughes, Chad M Landis, and Clemens V Verhoosel. A higher-order phase-field model for brittle fracture: Formulation and analysis within the isogeometric analysis framework. *Computer Methods in Applied Mechanics and Engineering*, 273:100–118, 2014.

[DHLK19] Zhiwen Deng, Chuangxin He, Yingzheng Liu, and Kyung Chun Kim. Super-resolution reconstruction of turbulent velocity fields using a generative adversarial network-based artificial intelligence framework. *Physics of Fluids*, 31(12):125111, 2019.

[EAK+20] Soheil Esmaeilzadeh, Kamyar Azizzadenesheli, Karthik Kashinath, Mustafa Mustafa, Hamdi A Tchelepi, Philip Marcus, Mr Prabhat, Anima Anandkumar, et al. Meshfreeflownet: a physics-constrained deep continuous space-time super-resolution framework. In *SC20: International Conference for High Performance Computing, Networking, Storage and Analysis*, pages 1–15. IEEE, 2020.

[FFT19] Kai Fukami, Koji Fukagata, and Kunihiko Taira. Super-resolution analysis with machine learning for low-resolution flow data. In *11th International Symposium on Turbulence and Shear Flow Phenomena, TSFP 2019*, 2019.

[FFT21] Kai Fukami, Koji Fukagata, and Kunihiko Taira. Machine-learning-based spatio-temporal super resolution reconstruction of turbulent flows. *Journal of Fluid Mechanics*, 909, 2021.

[GSW20] Han Gao, Luning Sun, and Jian-Xun Wang. Phygeonet: Physics-informed geometry-adaptive convolutional neural networks for solving parametric pdes on irregular domain. *arXiv e-prints*, pages arXiv–2004, 2020.

[GSW21] Han Gao, Luning Sun, and Jian-Xun Wang. Super-resolution and denoising of fluid flow using physics-informed convolutional neural networks without high-resolution labels. *Physics of Fluids*, 33(7):073603, 2021.

[KB15] Diederik P. Kingma and Jimmy Ba. Adam: A Method for Stochastic Optimization. *ICLR*, 2015.

[Key81] Robert Keys. Cubic convolution interpolation for digital image processing. *IEEE transactions on acoustics, speech, and signal processing*, 29(6):1153–1160, 1981.

[KT08] M. Kuroda and V. Tvergaard. A finite deformation theory of higher-order gradient crystal plasticity. *Journal of the Mechanics and Physics of Solids*, 56(8):2573–2584, 2008.

[LNN19] J. Lynggaard, K. L. Nielsen, and C. F. Niordson. Finite strain analysis of size effects in wedge indentation into a face-centered cubic (fcc) single crystal. *European Journal of Mechanics / A Solids*, 76:193–207, 2019.

[NN19] K. L. Nielsen and C. F. Niordson. A finite strain fe-implementation of the fleck-willis gradient theory: Rate-independent versus visco-plastic formulation. *European Journal of Mechanics / A Solids*, 75:389–398, 2019.

[NT19] C. F. Niordson and V. Tvergaard. A homogenized model for size-effects in porous metals. *Journal of the Mechanics and Physics of Solids*, 123:222–233, 2019.

[PGM+19] Adam Paszke, Sam Gross, Francisco Massa, Adam Lerer, James Bradbury, Gregory Chanan, Trevor Killeen, Zeming Lin, Natalia Gimelshein, Luca Antiga, Alban Desmaison, Andreas Kopf, Edward Yang, Zachary DeVito, Martin Raison, Alykhan Tejani, Sasank Chilamkurthy, Benoit Steiner, Lu Fang, Junjie Bai, and Soumith Chintala. Pytorch: An imperative style, high-performance deep learning library. In H. Wallach, H. Larochelle, A. Beygelzimer, F. d'Alché-Buc, E. Fox, and R. Garnett, editors, *Advances in Neural Information Processing Systems 32*, pages 8024–8035. Curran Associates, Inc., 2019.

[RPK17] Maziar Raissi, Paris Perdikaris, and George Em Karniadakis. Physics informed deep learning (part i): Data-driven solutions of nonlinear partial differential equations. *arXiv preprint arXiv:1711.10561*, 2017.

[RPK19] Maziar Raissi, Paris Perdikaris, and George E Karniadakis. Physics-informed neural networks: A deep learning framework for solving forward and inverse problems involving nonlinear partial differential equations. *Journal of Computational Physics*, 378:686–707, 2019.

[RSL21] Chengping Rao, Hao Sun, and Yang Liu. Physics-informed deep learning for computational elastodynamics without labeled data. *Journal of Engineering Mechanics*, 147(8):04021043, 2021.

[SW20] Luning Sun and Jian-Xun Wang. Physics-constrained bayesian neural network for fluid flow reconstruction with sparse and noisy data. *Theoretical and Applied Mechanics Letters*, 10(3):161–169, 2020.

[SWB+20] Akshay Subramaniam, Man Long Wong, Raunak D Borker, Sravya Nimmagadda, and Sanjiva K Lele. Turbulence enrichment using physics-informed generative adversarial networks. *arXiv preprint arXiv:2003.01907*, 2020.

[VDDP18] Athanasios Voulodimos, Nikolaos Doulamis, Anastasios Doulamis, and Eftychios Protopapadakis. Deep learning for computer vision: A brief review. *Computational intelligence and neuroscience*, 2018, 2018.

[XFCT18] You Xie, Erik Franz, Mengyu Chu, and Nils Thuerey. tempogan: A temporally coherent, volumetric gan for super-resolution fluid flow. *ACM Transactions on Graphics (TOG)*, 37(4):1–15, 2018.

[YZL+16] Gao Yingjun, Luo Zhirong, Huang Lilin, Mao Hong, Huang Chuanggao, and Lin Kui. Phase field crystal study of nano-crack growth and branch in materials. *Modelling and Simulation in Materials Science and Engineering*, 24(5):055010, 2016.

[ZBLN97] Ciyou Zhu, Richard H Byrd, Peihuang Lu, and Jorge Nocedal. Algorithm 778: L-bfgs-b: Fortran subroutines for large-scale bound-constrained optimization. *ACM Transactions on mathematical software (TOMS)*, 23(4):550–560, 1997.

[ZTK+18] Yulun Zhang, Yapeng Tian, Yu Kong, Bineng Zhong, and Yun Fu. Residual dense network for image super-resolution. In *Proceedings of the IEEE conference on computer vision and pattern recognition*, pages 2472–2481, 2018.